Materials Research Proceedings 41 (2024) 2839-2849 https://doi.org/10.21741/9781644903131-311

Investigation of the reshaping process by hydroforming using magnetorheological fluids

PICCININNI Antonio[1,a*], CUSANNO Angela[1,b], INGARAO Giuseppe[2,c], PALUMBO Gianfranco[1,d] and FRATINI Livan[2,e]

[1]Dept. of Mechanics, Mathematics and Management, Politecnico di Bari, Via Orabona 4, 70125 Bari

[2] Department of Engineering, University of Palermo, Viale delle Scienze, Palermo, 90128, Italy

[a]antonio.piccininni@poliba.it, [b]angela.cusanno@poliba.it, [c]giuseppe.ingarao@unipa.it, [d]gianfranco.palumbo@poliba.it, [e]livan.fratini@unipa.it

Keywords: Aluminium, Reshaping, Hydroforming, Magnetorheological Fluids

Abstract. The reshaping of End-of-Life (EoL) components is considered a promising approach to put in practice one of the virtuous strategies of the Circular Economy. The heterogeneity in a EoL part, the alternation of deformed/undeformed regions resulting from the manufacturing process, may hinder an effective reshaping into a brand new geometry. Therefore, the proper selection among the sheet metal forming processes to overcome such a limitation is of utmost importance. The present work, based on a full numerical approach, investigates the reshaping process of a disc-shaped EoL by hydroforming using a Magneto Rheological Fluid (MRF) as the forming medium. The basic idea is to combine the advantages coming from the flexibility of the hydroforming process with those from the MRF whose behavior (i.e. its viscosity affecting the shear stresses at the contact with the blank) can be tailored by adjusting the applied magnetic field. The reshaping approach is investigated according to two separate routes, differentiated by a different target geometry. A factorial plan of numerical simulations allowed to investigate the effect of the MRF behaviour as well as the geometry of the EoL component on the quality of the reshaped part, expressed in terms of accuracy in the final shape and thickness distribution.

Introduction

The production of the five key materials (aluminum, steel, cement, paper, and plastic) is responsible for more than 50% of emitted greenhouse gases (GHG) each year [1]. Primary aluminum production is the most energy and emissions intensive among the aforementioned materials [2]. The main approach for reducing the primary production and decoupling the resource depletion from the economic growth is the implementation of Circular Economy Strategies [3]. Turning End-of-Life (EoL) products/components directly into new products/components is considered a promising route to be investigated. Remanufacturing and Reshaping are considered two strategies, among the five enlisted by Cooper and Allwood [4], to reuse EoL in line with the pillars of the Circular Economy. At the same time, it should be pointed out that a successful application of the Remanufacturing/Reshaping strategies needs the choice of innovative processes or, alternatively, the re-design of the conventional ones. Moreover, sheet metal based accounts for a large share of the semi-finished product: thus, investigating new reuse solution for sheet metal based EoL components would be of utmost importance. As it is documented in the scientific literature, flexible sheet metal forming processes are ideal candidate to put in practice the principle of the Reshaping, being also able to overcome the limitation coming from an already deformed EoL component. As an example, Brosius et al. [5] describe the reshaping of a car hood into a rectangular sheet metal component by the hydroforming process. Takano et al. [6], once flattened a bent sheet, applied the Single Point Incremental Forming (SPIF) to reshape the blank into a new

geometry. Recently, the authors of the present paper proposed a new Reshaping approach based on the Sheet Hydroforming (SHF) process: blanks with a square deep drawn feature located in different positions was successfully reshaped according to a new brand benchmark geometry [7]. Nevertheless, the research for process variants allowing to further improve the performance of the SHF process is still an open question: as an example, MagnetoRheological Pressure Forming (MRPF) is gaining interest since the thickness and the strain distribution on the formed part can be affected by properly changing the properties of the forming medium [8]. In the case of MRPF, the forming medium is a MagnetoRheological Fluid (MRF), that is based on a suspension of magnetically responsive particles in a liquid carrier, whose rheological behaviour (e.g., its viscosity) can be changed quickly and reversibly if subjected to a magnetic field [9]. MRFs are currently used in the automotive field for brakes [10] and clutches [11], but also in sheet metal forming applications [12]. In the present work the adoption of a MRF as the forming medium in a reshaping approach by sheet hydroforming was numerically simulated. The aim is to evaluate to what extent the variation in the MRF behaviour (due to the change in the applied magnetic field) allows to effectively reshape an EoL component represented by a circular blank with a deep drawn feature. The main influencing parameters (those related to the geometrical properties of the deep drawing feature and those related to the MRF behaviour) were changed according to a factorial plan to evaluate how they affected the final shape and thickness distribution of the reshaped part. In order to make the approach more general, the reshaping was simulated according to two different targets, a frustum-shaped geometry and a hemispherical one.

Methodology

The reshaping approach by SHF adopting a MRF as the forming media was simulated according to two different routes: (i) the first one, indicated as ROUTE#1, is based on an initial deep drawing step to obtain the EoL component that is subsequently forced to copy a truncated cone die (see Fig. 1a); (ii) in the second one (indicated as ROUTE#2), the same EoL by deep drawing is deformed by the MRF in a free-bulging-like condition up to a target height (see Fig. 1b).

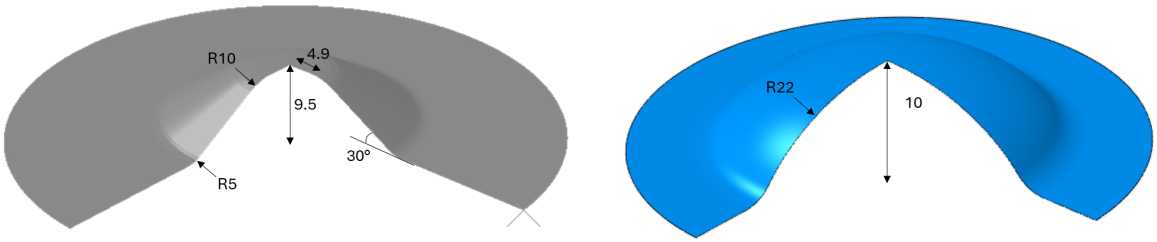

a) b)

Fig. 1 The reshaping approach: a) target die for the ROUTE#1, b) target shape for the ROUTE#2 (dimensions are in mm)

FE model of the reshaping routes. The whole process was simulated using the FE commercial code Abaqus (v2017) and was based on two consecutive steps (both were solved using the dynamic implicit solver). By taking advantages from a 2D axisymmetric approach, the circular blank was initially deformed by deep drawing (to obtain the EoL component) and subsequently reshaped by the action of the MRF. The two investigated approaches are resumed in Fig. 2.

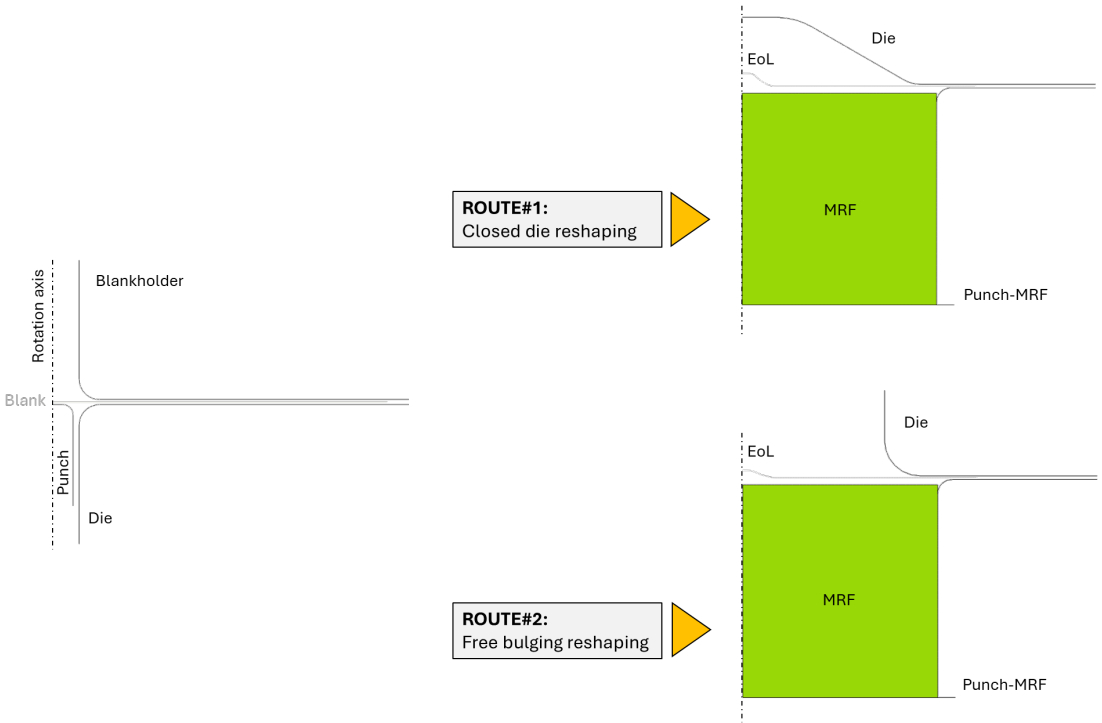

Fig. 2 Overview of the two investigated Reshaping routes

Regardless of the investigated route, the first step to obtain the EoL component was simulated by modelling the tools (punch, blankholder and die) as analytical rigid wire-based bodies and the blank as a shell deformable body (initial diameter of 66 mm and thickness of 0.5 mm). The blank was discretized by means of 0.1 mm SAX1 (2 nodes, one-point integration) elements. Contacts pairs between the blank and the tools were modelled as surface-to-surface component, setting the friction coefficient of 0.1 (penalty formulation). Material data of the blank (flow curve and limit forming curve) were taken from literature [7]. As for the reshaping step, the MRF was modelled as a solid axisymmetric body and discretized by means of 3300 CAX4H (4-node bilinear, hybrid with constant pressure) elements whose size was progressively refined (from 1 to 0.25 mm) in proximity of the contact with the EoL. The MRF was modelled as purely elastic body and material data (Young's modulus and Poisson's ratio) expressed as a function of the applied magnetic field (the determination of the elastic properties is detailed in [13]). The MRF exerted its action on the blank because of the vertical displacement of a punch (indicated as *Punch-MRF* in Fig. 1) modelled as an analytical rigid body (as the other tools). During the reshaping step, the blank peripheral node was completely constrained (thus mainly inducing a stretching-based deformation mechanism).

FE simulation of different reshaping scenarios. The effectiveness of the reshaping step, in terms of overall quality of the final component, was judged to be mainly dependent on the value of the applied magnetic field (that, in turns, affects the MRF behaviour) and on the geometry of EoL part (basically, the geometric properties of the deep drawn feature). Therefore, a factorial plan of 25 simulations was created based on a Central Composite Design by varying the following set of parameters: (i) the radial position of punch during the deep drawn (indicated by r in Fig. 3), (ii) the diameter of the punch (indicated by d_p in Fig. 3), (iii) the punch stroke during the deep drawing step (h) and (iv) the applied magnetic field (B).

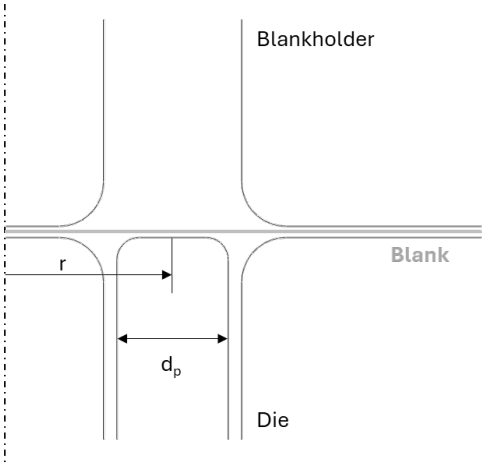

Fig. 3 Geometrical parameters affecting the deep drawn feature.

The mentioned quantities were varied within their relative variation ranges, listed in Table 1.

Table 1 Intervals range of the input parameters

Input parameter	Lower Bound	Upper Bound
r	0 mm	15 mm
d_p	4 mm	6 mm
h	1 mm	1.8 mm
B	0 mT	3.8 mT

The results of each simulation were analyzed in terms of error-based response outputs to evaluate the effectiveness of the reshaping step. More in details, the two error functions were meant to quantify the average percentage deviation in terms of thickness distribution (Eq. 1) and final shape (Eq. 2). The reference case, against which the two error functions were calculated, was: (i) the deformed blank only by the action the MRF (in absence of applied magnetic field) for the ROUTE#1 and (ii) the target geometry shown in Fig. 1b for the ROUTE#2.

$$Err_{avg,th}[\%] = \frac{1}{N}\sum_{i=1}^{N}\left(\frac{t_{i,ref} - t_{i,comp}}{t_{i,ref}} \cdot 100\right) \quad (1)$$

$$Err_{avg,sh}[\%] = \frac{1}{N}\sum_{i=1}^{N}\left(\frac{u_{i,ref} - u_{i,comp}}{u_{i,ref}} \cdot 100\right) \quad (2)$$

The subscripts *ref* and *comp* refer to the quantities (nodal thickness *t* and displacement *u*) extracted from the reference case and from each simulated condition, respectively; *N* is the total number of nodes discretizing the blank. The plan of 25 simulations was simulated for both the reshaping routes.

Results and discussion

Reshaping ROUTE#1. The table containing the input and the response values from each of the simulated conditions was imported into the working environment of the integration platform modeFRONTIER (v 2023R3). The values of the two response variables were fitted by means of interpolating Response Surfaces (RS) trained by means of Radial Basis Functions (RBF). In order to choose the most effective kernel (among Hardy's MultiQuadrics, Inverse MultiQuadrics, Gaussians, Duchon's Polyharmonic Splines and Wendland's Compactly Supported), data were split into two subgroups: the training set (generally containing between 80% and 90% of the whole

set) that is used to actually train the RS and the validation set (containing the remaining part of the data table) used to evaluate the predictive capability of the trained model. The $Err_{avg,sh}$ and $Err_{avg,th}$ were accurately fitted by the RBF Gaussian and Hardy's MultiQuadrics kernels, respectively.

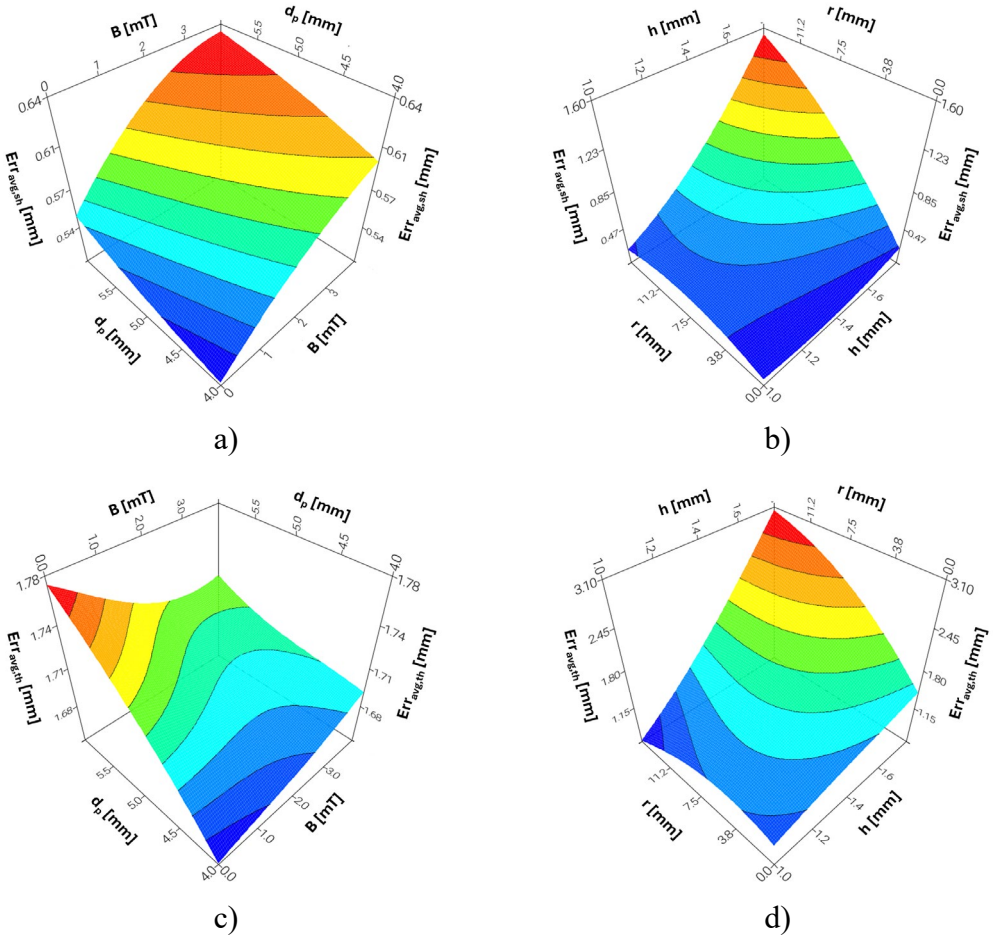

Fig. 4 Reshaping ROUTE#1: RS on the response variable $Err_{avg,sh}$ (a, b) and on the response variable $Err_{avg,th}$ (c, d).

The 3D visualization of the regression model in Fig. 4a suggests that the final geometry of the reshaped part was slightly influenced by the punch diameter used during the deep drawing step: setting, in fact, the d_p at 4 mm the error variable is weakly influenced. Similarly, the applied magnetic field showed an almost negligible influence as well. On the other hand, as shown by the RS in Fig. 4b, the final shape got less accurate when increasing the punch stroke and/or moving the deep drawn feature far from the rotation axis (r equal to 15 mm). Such a consideration was justified by the fact that blank's region far from the rotation axis were subjected to lower strain levels since almost immediately in contact with the inclined segment of the die. As an example, the final shape of the ID6 and ID7 was compared with the reference target: if the deep drawn feature is located at the center of the blank, the reshaped part shows only small variation in its flat part (see the detailed plot Fig. 5a). Moving the strain inhomogeneity far from the rotation axis, on the other hand, affects the shape of the whole tapered surface of the reshaped part (the green and black curves are not completely overlapped (see Fig. 5b).

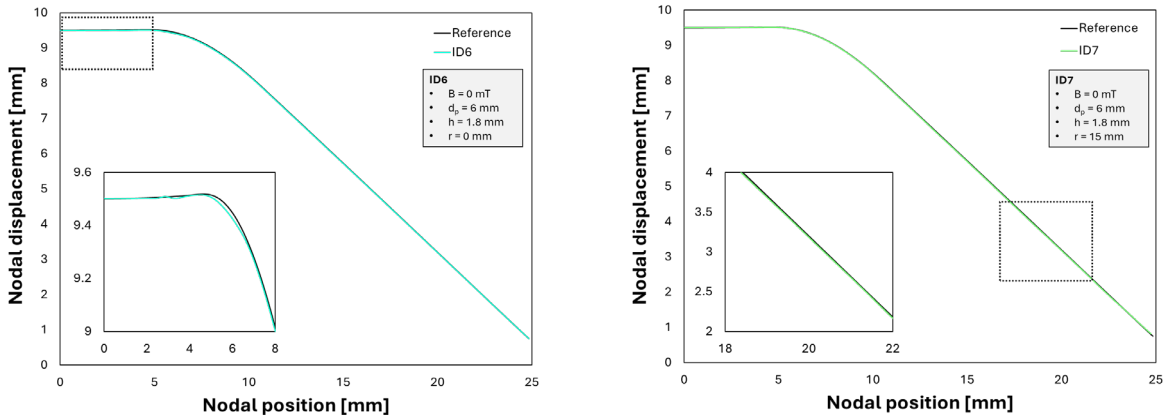

a) b)

Fig. 5 Influence of the parameter "r" on the final geometry of the reshaped part

On the other hand, when looking at the deviation of the final thickness distribution in the reshaped part from the target one (see Fig. 4c and Fig. 4d), similar conclusions could be drawn. In fact, the heterogeneity resulting from the deep drawing could not be completely eliminated during the reshaping even if the deep drawn feature was located close to the center of the blank (see Fig. 6a); as expected, by moving the feature close to the peripheral region of the blank, the residual heterogeneity in the thickness distribution of the reshaped part was even more evident (see Fig. 6b).

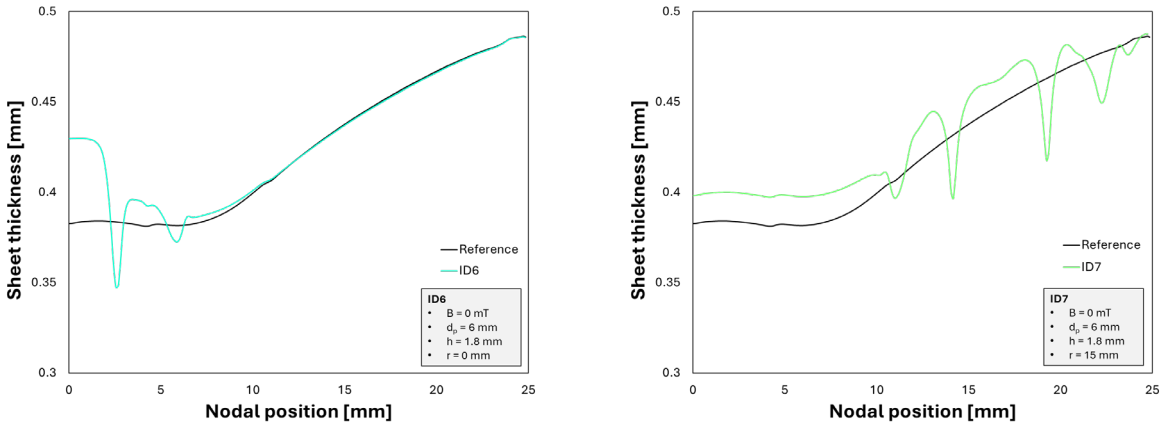

a) b)

Fig. 6 Influence of the parameter "r" on the final thickness distribution of the reshaped part

Eventually, by looking at the main effect plots in Fig. 7 (a and b), it could be concluded that, when reshaping the EoL component in a closed die, the depth (*h*) and the radial position (*r*) of the deep drawn feature showed a much larger influence on the final shape and thickness distribution (in accordance with what reported in [7]).

a)

b)

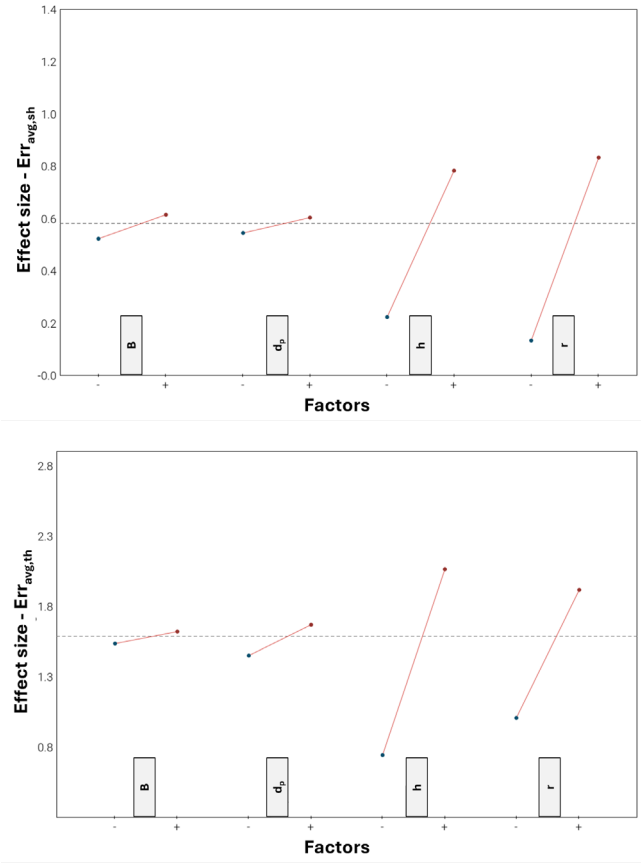

Fig. 7 Reshaping ROUTE#1: main effect plots on $Err_{avg,sh}$ (a) and $Err_{avg,th}$ (b)

Reshaping ROUTE#2. The same approach was used also to analyze the results from the second DoE plan. The 3D visualization of the regression models (Hardy's MultiQuadrics kernel on the $Err_{avg,sh}$ variable and Inverse MultiQuadrics kernel on the $Err_{avg,th}$ variable) suggests that the successful reshaping of the EoL into the target geometry was strictly related to the applied magnetic field (Fig. 8a). Also in this case, the radial position of the deep drawn feature influences the final geometry of the reshaped component (Fig. 8a).

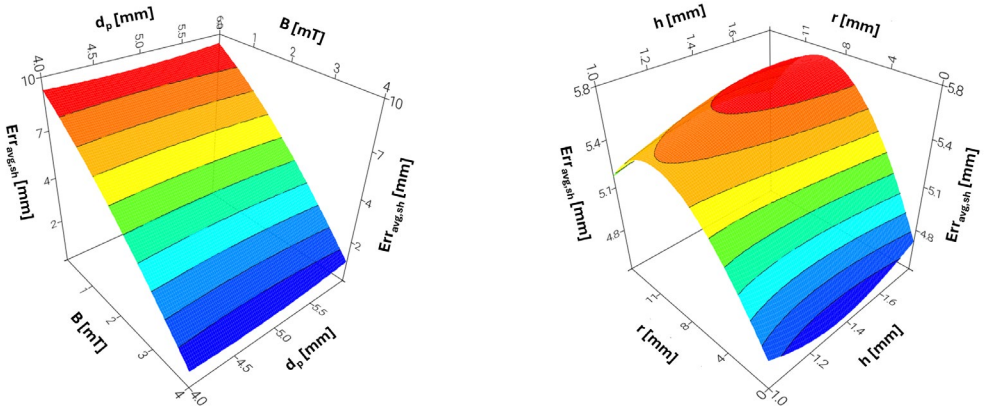

a) b)

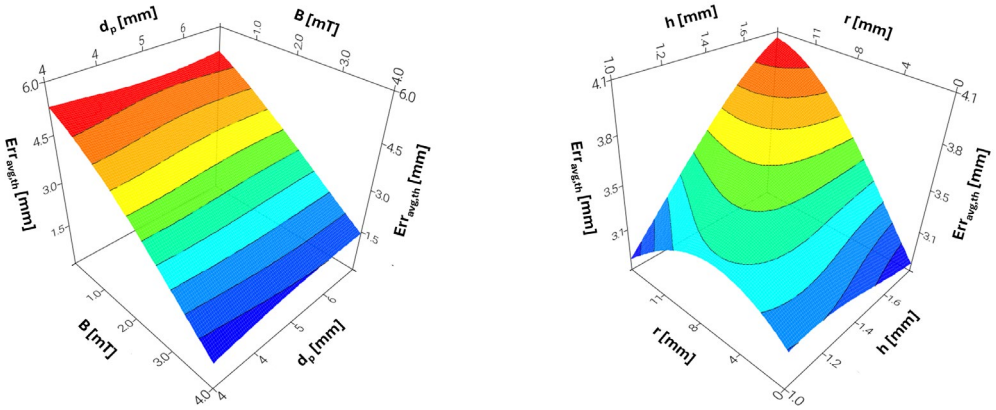

c) d)

Fig. 8 Reshaping ROUTE#2: RS on the response variable $Err_{avg,sh}$ (a, b) and on the response variable $Err_{avg,th}$ (c, d).

In order to deepen more the effect of the applied magnetic field (*B*), ID6 and ID14 were compared with the target geometry: the comparison in Fig. 9a clearly suggest that, for the same displacement of the plate moving the MRF (*Punch-MRF* in Fig. 2), the reshaping step was less effective if no magnetic field was applied (B equal to 0 mT). On the contrary, the increased fluid viscosity resulting from the increase of the magnetic field *B* allowed to obtain a final shape almost completely overlapped to the target one (Fig. 9b).

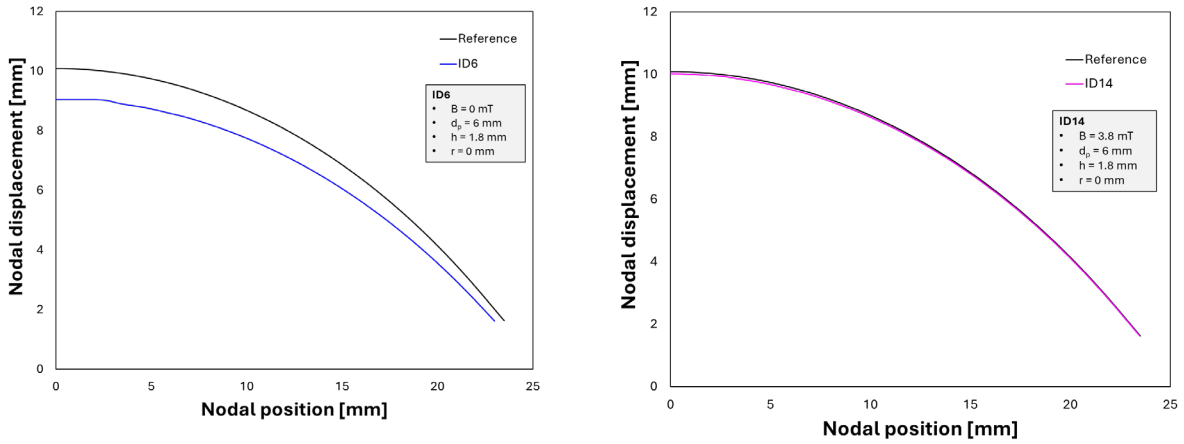

a) b)

Fig. 9 Influence of the parameter "B" on the final geometry of the reshaped part

In the case of the final thickness distribution (the RS are shown in Fig. 8, c and d), an expected reduction of the discrepancy with the target distribution was achieved when increasing the magnetic field. The comparison of the curve demonstrates that, despite the difference close to the rotation axis (strictly related to the heterogeneously cold-worked regions after the deep drawing), the thickness distribution approximated better the target one thanks to the increased MRF viscosity (Fig. 10a). On the other hand, as a consequence of the lower final bulging height reached in absence of magnetic field, the final distribution was much less accurate (Fig. 10b).

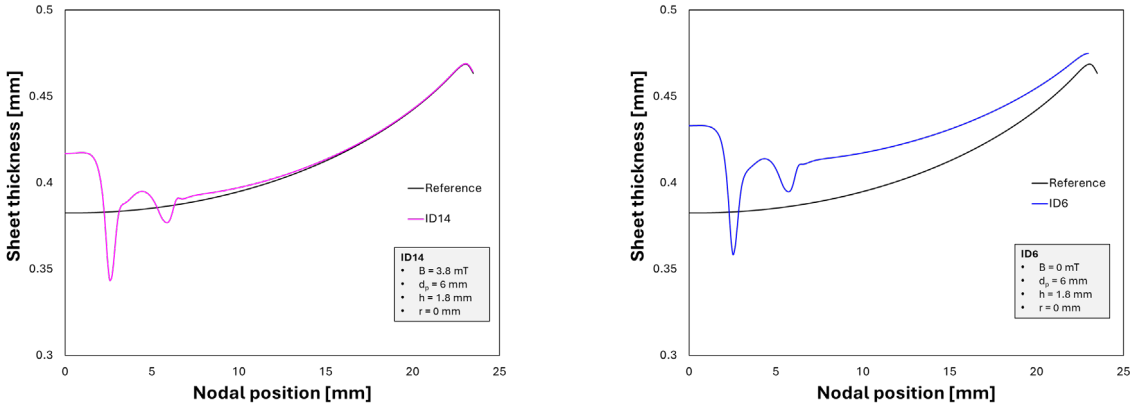

a) b)

Fig. 10 Influence of the parameter "B" on the final thickness distribution of the reshaped part

The analysis of the main effect plot (Fig. 11a) allowed to conclude that the parameter B remarkably influenced the two response variables. In particular, when dealing with deviation in the final thickness distribution, also the radial position of the deep drawn feature showed a non-negligible effect (Fig. 11a).

a)

b)

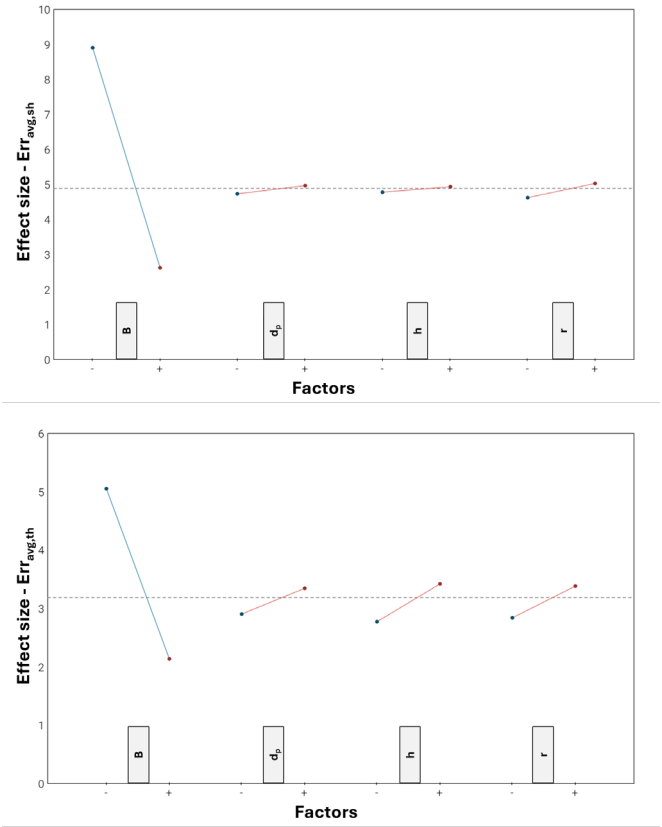

Fig. 11 Reshaping ROUTE#2: main effect plot

Conclusions

In the present work, the reshaping by hydroforming was studied including the investigation of the advantages coming from the adoption of a MRF as the forming medium. The key findings of the presented methodology as it follows: (i) a simple 2D axisymmetric model made possible to easily simulate the sequence of two manufacturing step: an initial deep drawing step to obtain the EoL component and the subsequent reshaping by MRF hydroforming; (ii) Taking into account two reshaping routes allowed to evaluate to what extent the process parameter of the deep drawing step

as well as the MRF behavior could have an influence according to the final target shape; (iii) in the case of the reshaping adopting a closed die (ROUTE#1), the *B* parameter had a negligible influence on the final quality of the reshaped part that, on the contrary, was much more dependent on the geometry of the EoL component (radial position and depth of the deep drawn feature); (iv) when changing the target geometry (ROUTE#2), the influence of the parameters changed completely: only an increase in the MRF viscosity (i.e. an increase in the applied magnetic field) allowed to obtain a reshaped part with a very accurate final shape and a thickness distribution close to the target values.

Acknowledgments
Financed by the European Union - NextGenerationEU (National Sustainable Mobility Center CN00000023, Italian Ministry of University and Research Decree n. 1033 - 17/06/2022, Spoke 11 - Innovative Materials & Lightweighting). The opinions expressed are those of the authors only and should not be considered as representative of the European Union or the European Commission's official position. Neither the European Union nor the European Commission can be held responsible for them.

References

[1] Oberhausen, G., Zhu, Y., and Cooper, D. R., 2022, "Reducing the Environmental Impacts of Aluminum Extrusion," Resour. Conserv. Recycl., **179**(December 2021), p. 106120. https://doi.org/10.1016/j.resconrec.2021.106120

[2] Ashby, M. F., 2021, "Materials and Environment," M.F.B.T.-M. and the E. (Third E. Ashby, ed., Butterworth-Heinemann, pp. 41–64. https://doi.org/10.1016/B978-0-12-821521-0.00003-7

[3] Tolio, T., Bernard, A., Colledani, M., Kara, S., Seliger, G., Duflou, J., Battaia, O., and Takata, S., 2017, "Design, Management and Control of Demanufacturing and Remanufacturing Systems," CIRP Ann., **66**(2), pp. 585–609. https://doi.org/10.1016/j.cirp.2017.05.001

[4] Cooper, D. R., and Allwood, J. M., 2012, "Reusing Steel and Aluminum Components at End of Product Life," Environ. Sci. Technol., **46**(18), pp. 10334–10340. https://doi.org/10.1021/es301093a

[5] Brosius, A., Hermes, M., Khalifa, N. Ben, Trompeter, M., and Tekkaya, A. E., 2009, "Innovation by Forming Technology: Motivation for Research," Int. J. Mater. Form., **2**(1), pp. 29–38. https://doi.org/10.1007/s12289-009-0656-9

[6] Takano, H., Kitazawa, K., and Goto, T., 2008, "Incremental Forming of Nonuniform Sheet Metal: Possibility of Cold Recycling Process of Sheet Metal Waste," Int. J. Mach. Tools Manuf., **48**(3), pp. 477–482. https://doi.org/10.1016/j.ijmachtools.2007.10.009

[7] Piccininni, A., Cusanno, A., Palumbo, G., Zaheer, O., Ingarao, G., and Fratini, L., 2022, "Reshaping End-of-Life Components by Sheet Hydroforming: An Experimental and Numerical Analysis," J. Mater. Process. Technol., **306**(June), p. 117650. https://doi.org/10.1016/j.jmatprotec.2022.117650

[8] Wang, P. yi, Zhang, W. zhuo, Wang, Z. jin, and Yi, J., 2016, "Effect of Viscosity of Viscous Medium on Formability of Al1060-O Sheet in Viscous Pressure Forming (VPF): An Experimental Study," Int. J. Adv. Manuf. Technol., pp. 1–10. https://doi.org/10.1007/s00170-016-8429-3

[9] Zhu, X., Jing, X., and Cheng, L., 2012, "Magnetorheological Fluid Dampers: A Review on Structure Design and Analysis," J. Intell. Mater. Syst. Struct., **23**(8), pp. 839–873. https://doi.org/10.1177/1045389X12436735

[10] Kumbhar, B. K., Patil, S. R., and Sawant, S. M., 2015, "Synthesis and Characterization of

Magneto-Rheological (MR) Fluids for MR Brake Application," Eng. Sci. Technol. an Int. J., **18**(3), pp. 432–438. https://doi.org/10.1016/j.jestch.2015.03.002

[11] Bucchi, F., Forte, P., and Frendo, F., 2012, "Experimental Characterization of a Permanent Magnet Magnetorheological Clutch for Automotive Applications," ASME 2012 11th Bienn. Conf. Eng. Syst. Des. Anal. ESDA 2012, **4**, pp. 345–355. https://doi.org/10.1115/ESDA2012-82284

[12] Li, F., Zhou, F. J., Wang, M. N., Zhu, S. Y., and Jin, C. C., 2017, "New Processing Research on Sheet Metal Bidirectional Pressure Forming Using a Magnetorheological Fluid," Int. J. Adv. Manuf. Technol., **88**(1–4), pp. 923–929. https://doi.org/10.1007/s00170-016-8831-x

[13] Cusanno, A., Piccininni, A., Guglielmi, P., and Palumbo, G., 2022, "Evaluation of the Rheological Behaviour of Magnetorheological Fluids Combining Bulge Tests and Inverse Analysis," *Key Engineering Materials*, Trans Tech Publications Ltd, pp. 1778–1785. https://doi.org/10.4028/p-4irh1n